

The Surprising Transparency of the sQGP at LHC

W. A. Horowitz*

*Department of Physics, University of Cape Town,
Private Bag X3, Rondebosch 7701, South Africa*

Miklos Gyulassy

*Department of Physics, Columbia University,
538 West 120th Street, New York, NY 10027, USA*

(Dated: July 7, 2018)

We present parameter-free predictions of the nuclear modification factor, $R_{AA}^\pi(p_T, s)$, of high p_T pions produced in Pb+Pb collisions at $\sqrt{s_{NN}} = 2.76$ and 5.5 ATeV based on the WHDG/DGLV (radiative+elastic+geometric fluctuation) jet energy loss model. The initial quark gluon plasma (QGP) density at LHC is constrained from a rigorous statistical analysis of PHENIX/RHIC π^0 quenching data at $\sqrt{s_{NN}} = 0.2$ ATeV and the charged particle multiplicity at ALICE/LHC at 2.76 ATeV. Our perturbative QCD tomographic theory predicts significant differences between jet quenching at RHIC and LHC energies, which are qualitatively consistent with the p_T -dependence and normalization—within the large systematic uncertainty—of the first *charged* hadron nuclear modification factor, R_{AA}^{ch} , data measured by ALICE. However, our constrained prediction of the central to peripheral pion modification, $R_{cp}^\pi(p_T)$, for which large systematic uncertainties associated with unmeasured p+p reference data cancel, is found to be over-quenched relative to the charged hadron ALICE R_{cp}^{ch} data in the range $5 < p_T < 20$ GeV/c. The discrepancy challenges the two most basic jet tomographic assumptions: (1) that the energy loss scales linearly with the initial local comoving QGP density, ρ_0 , and (2) that $\rho_0 \propto dN^{ch}(s, \mathcal{C})/dy$ is proportional to the observed global charged particle multiplicity per unit rapidity as a function of \sqrt{s} and centrality class, \mathcal{C} . Future LHC identified ($h = \pi, K, p$) hadron R_{AA}^h data (together with precise p+p, p+Pb, and Z boson and direct photon Pb+Pb control data) are needed to assess if the QGP produced at LHC is indeed less opaque to jets than predicted by constrained extrapolations from RHIC.

PACS numbers: 12.38.Mh, 24.85.+p, 25.75.-q

Keywords: QCD, Relativistic heavy-ion collisions, Quark gluon plasma, Jet quenching, Jet Tomography

I. INTRODUCTION

The first LHC Pb+Pb data at $\sqrt{s} = 2.76$ ATeV [1–6] provide important new consistency tests of dynamical models developed over the past two decades to predict multiparticle observables in nuclear reactions at $\sqrt{s} = 0.2$ AGeV from the Relativistic Heavy Ion Collider (RHIC/BNL) [7–10]. The new LHC energy frontier with Pb+Pb probes the physics of strongly coupled Quark Gluon Plasma (sQGP) [11–13] at densities approximately twice as high as at RHIC, with temperatures up to $T \sim 500$ MeV, well above the deconfinement transition region predicted by lattice QCD [14, 15].

The theoretical understanding of the dynamical properties of this new form of matter is however far from complete. On the one hand, bulk radial and differential azimuthal anisotropic elliptic flow data of low transverse momenta ($p \sim 3T_0 \approx 1$ GeV) partons were found to be consistent with near “perfect fluid” flow and suggest highly nonperturbative physics of this new form of matter

[16, 17]. This has led to proposals that the bulk properties of the sQGP may be better approximated via strong coupling (supergravity dual) holography models [18–29] than via perturbative QCD (pQCD) based quark and gluon quasiparticle Hard Thermal Loop (HTL) [30, 31] approximations.

On the other hand, short wavelength ($p_T \sim 10 - 20$ GeV/c) properties of the sQGP, as measured via the nuclear modification factor of pions [32–34], were found to be well predicted by pQCD based HTL partonic radiative energy loss theory [35–57]. The nuclear modification factor of high transverse momentum hadron, h , fragments in $A + B \rightarrow h + X$ and centrality class \mathcal{C} used to probe the short wavelength dynamics in an sQGP is defined as

$$R_{AB}^h(y, \vec{p}_T; \sqrt{s}, \mathcal{C}) = \frac{dN^{A+B \rightarrow h}(y, \vec{p}_T, \sqrt{s}, \mathcal{C})/dy d^2\vec{p}_T}{T_{AB}(\mathcal{C}) d\sigma^{p+p \rightarrow h}(\sqrt{s})/dy d^2\vec{p}_T}. \quad (1)$$

For a fixed \sqrt{s} center of mass (cm) energy (per nucleon pair) and nucleon-nucleon (NN) inelastic cross section $\sigma_{NN}^{in}(\sqrt{s})$ the mean number of elementary binary NN collisions in centrality class \mathcal{C} is given by $\sigma_{NN}^{in} T_{AA}$, where

* wa.horowitz@uct.ac.za

[58]

$$T_{AB}(\mathcal{C}) = \left\langle \int d^2\vec{x}_\perp T_A(\vec{x}_\perp - \frac{\vec{b}}{2}) T_B(\vec{x}_\perp + \frac{\vec{b}}{2}) \right\rangle_{b \in \mathcal{C}} \quad (2)$$

in terms of the Glauber nuclear thickness profile $T_A(\vec{x}_\perp) = \int dz \rho_A(z, \vec{x}_\perp)$ and Wood-Saxon nuclear density ρ_A normalized to A .

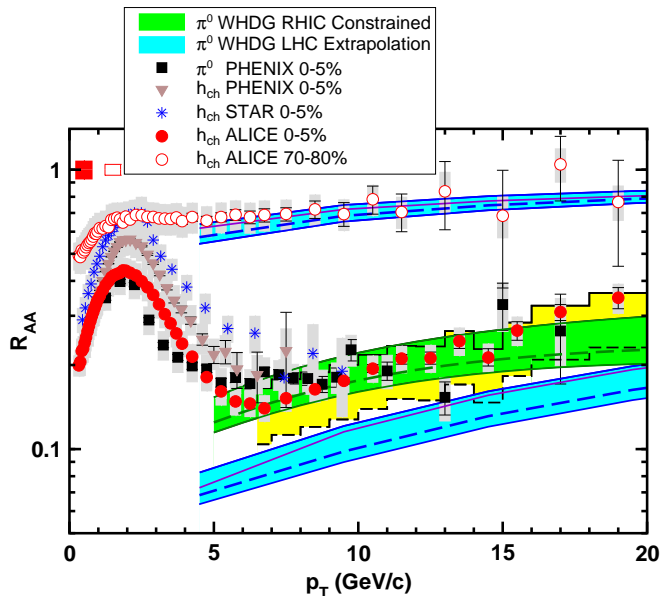


FIG. 1. WHDG model [53] predictions (blue bands extrapolated from the RHIC constrained green band) for the nuclear modification factor of π^0 in Pb+Pb 2.76 ATeV LHC are compared to ALICE/LHC [1] charged hadron nuclear modification data in central (red solid) and peripheral (open red) reactions. The PHENIX/RHIC Au+Au $\rightarrow \pi^0$ nuclear modification data [34] are shown by black dots. The brown triangles and blue stars represent the charged hadron PHENIX [32] and STAR [33] data, respectively. The blue band of WHDG predictions corresponds to the $1-\sigma$ medium constraint set by PHENIX [34] extrapolated to LHC via the ALICE charged particle rapidity density [2]. The wide yellow band is the current systematic error band of the (red dot) LHC data due to the unmeasured $p+p$ reference denominator.

In the absence of both initial state and final state nuclear interactions $R_{AB} = 1$. For p_T below some characteristic medium dependent transverse momentum “saturation” scale, $Q_s(p_T, \sqrt{s}, A)$, the initial nuclear partonic distributions functions (PDFs) [59–61] $f_{a/A}(x = 2p_T/\sqrt{s}, Q^2 \sim p_T^2) < A f_{a/N}(x, Q^2)$ are expected to be shadowed, leading to $R_{AA} < 1$ because the incident flux of partons is less than A times the free nucleon parton flux. Color Glass Condensate (CGC) models [11, 62–68] have been developed to predict $Q_s(p_T, \sqrt{s}, A)$ related initial state effects from first principles. While the magnitude of Q_s at LHC is uncertain and will require future dedicated $p+Pb$ control measurements to map out, current expectations are that $Q_s < 5$ GeV at LHC in the central rapidity region. This should leave a wide jet to-

mographic kinematic window $10 < p_T < 200$ GeV in which nuclear modification should be dominated by final state parton energy loss and broadening effects. In this paper, we therefore assume that initial state nuclear effects can be neglected in the $10 < p_T < 20$ (i.e. $x > 0.01$) range explored by the first ALICE data [1]. We note that from Fig. 1, and as discussed in detail below, our RHIC constrained jet quenching due to final state interactions alone already tends to over-predict the pion quenching at LHC and therefore leaves no room for large additional shadowing/saturation effects in the [68–70] in this $Q^2 > 100$ GeV² kinematic window—unless the sQGP is much more transparent at LHC than expected from most extrapolations of jet quenching phenomena from SPS and RHIC to LHC energies.

The main challenge to pQCD multiple collision theory of jet tomography and AdS/CFT jet holography is how to construct a consistent approximate framework that can account simultaneously for the beam energy dependence from SPS to LHC energy and for the nuclear system size, momentum, and centrality dependence from $p+p$ to $U+U$ of four major classes of hard probe observables: (1) the light quark and gluon leading jet quenching pattern as a function of the resolution scale p_T , (2) the heavy quark flavor dependence of jet flavor tagged observables, and (3) the azimuthal dependence of high p_T particles relative to the bulk reaction plane determined from low- p_T elliptic flow and higher azimuthal flow moments, $v_n(p_T)$, and (4) corresponding di-jet observables.

The first LHC heavy ion data on high transverse momentum spectra provide an important milestone because they test for the first time the density or opacity dependence of light quark and gluon jet quenching theory in a parton density range approximately twice as large as that studied at RHIC. The surprise from LHC is the relatively small difference observed between the RHIC [32–34] and ALICE [1] LHC data on $R_{AA}(10 < p_T < 20$ GeV), as shown in Fig. 1. In addition, there is little difference from RHIC to LHC between the differential elliptic flow probe, $v_2(p_T < 2)$, as reported in [3]. The rather striking similarities between bulk and hard observables at RHIC and LHC pose significant consistency challenges for both initial state production and dynamical modeling of the sQGP phase of matter.

In this paper, we focus on the puzzle posed by the similarity of inclusive light quark/gluon jet quenching at RHIC and LHC by performing a constrained extrapolation from RHIC using the WHDG model [53] to predict $R_{AA}^{\pi^0}$ at 2.76 ATeV cm energy. We update our earlier 2007 LHC predictions in [71, 72], by extrapolating the 2008 $1-\sigma$ PHENIX/RHIC constraints [34] of the opacity range at $\sqrt{s} = 0.2$ ATeV using the new 2.76 ATeV ALICE/LHC [2, 4] charged hadron rapidity density data, $dN_{ch}/d\eta = 1601 \pm 60$, in the 0–5% most central collisions and 35 ± 2 in the 70–80% peripheral collisions.

We note that in strong coupling AdS/CFT approaches to hard jet probes, the pQCD high- p_T jet tomography theory is replaced by a gravity dual jet holographic

model. That approach is based on the assumption that the 't Hooft coupling, $\lambda \equiv 4\pi\alpha_s N_c$, as well as N_c are large enough that an approximate 10D supergravity dual description of the dynamics may be used. Jet quenching is then mapped into the problem of classical string drag over a black brane horizon in an AdS curved spacetime with an isometry group that is identical to the exact conformal symmetry group of the $\mathcal{N} = 4$ Supersymmetric Yang-Mills (SYM) cousin of QCD. The thermally equilibrated strongly coupled supersymmetric QGP is assumed dual to the black brane. In [73], it was shown that with $\lambda \sim 20$ and $N_c = 3$ ($\alpha_s \approx 0.5$) AdS/CFT holography provides a remarkably robust analytic account of both the single nonphotonic electron (heavy quark jet) quenching as well as bulk elliptic flow data, a simultaneous description of which has remained out of reach of perturbative QCD methods. However, the theoretical consistency of heavy quark jet holography remains controversial in the literature (see, e.g., [74]). Light jet holography of R_{AA}^{ch} is even more challenging. So far, only schematic falling strings scenarios have been proposed to address light quark/gluon quenching observables [26, 27]. However, high- p_T elliptic moment $v_2(p_T)$ phenomenology [75–78] appears to require nonlinear path length dependences, $L^{n \geq 3}$, more suggestive of falling string scenarios than $L^{n \leq 2}$ path dependences predicted by pQCD for static plasmas. Future heavy flavor tagged jet observables [73, 79–81] will help to discriminate between competing jet holography vs. perturbative tomography models of jet attenuation.

II. JET TOMOGRAPHY: QUALITATIVE

One feature common to both pQCD tomography and gravity dual holography is that both predict the energy loss per unit length, dE/dL , increases monotonically with the plasma density or temperature. In this section we consider a generic analytic energy loss that can interpolate between a wide range of dynamical scenarios and provide qualitative understanding of the quantitative numerical WHDG results presented in Section III.

Consider the following power law model for jet energy loss [78]

$$\frac{dP}{d\tau} = -\kappa P^a \tau^b T^{2-a+b}(x(\tau), \tau) \quad (3)$$

where $P(\tau)$ is the momentum (energy) of a massless jet passing through a plasma with a local temperature field $T(x, \tau)$. The solution for an initial energy $P(0)$ and jet path, $x(\tau)$, a uniform static “plasma brick” of thickness L is

$$\frac{P(L)}{P(0)} = \left(1 - \kappa(LT)^{1+b} \left(\frac{T}{P(0)} \right)^{1-a} \right)^{\frac{1}{1-a}}. \quad (4)$$

We note that $\partial P(0)/\partial P(L) = (P(0)/P(L))^a$ is the Jacobian of the transformation between $P(0)$ and $P(L)$. The

parameters a and b control the jet energy and path length dependence energy (momentum) loss per unit length (time) and fixes the power of the temperature or parton density $\rho \propto T^3$ dependence.

The thermal stopping distance L_T , as defined by $P(L_T) = P_T = T$, is then:

$$L_T(P_0, T, a, b, c) = \left(\frac{P_0^{1-a} - T^{1-a}}{(1-a)\kappa T^{2-a+b}} \right)^{\frac{1}{1-a}} \quad (5)$$

In pQCD, the opacity series WHDG/DGLV [42, 43, 47, 53] for a massless parton jet leads (in a static uniform plasma) to $dE_{GLV}/dL \approx -\kappa T^3 L^1 \log(E/T)$. Therefore $b = 1$ (or 0) in the LPM regime in static (or Bjorken expanding) plasmas. Because $E^{1/3}/\log(E) \approx 1 \pm 0.1$ in the range $5 < E/T < 200$, we can simulate pQCD light quark jet energy dependence with ($a \approx 1/3, b = 1$). The density dependence is then roughly linear with $T^{8/3} \sim \rho^{8/9}$ in the static case.

Another interesting limiting case in pQCD is for thick plasmas, where the deep LPM regime leads to the BDMS [45] formula, $dE_{BDMS}/dL = -\kappa E^{1/2} L^1 T^{5/2}$ that grows with density as $\rho^{5/6}$. Increasing the density by a factor equal to the ratio of charged particle multiplicities, ≈ 2.1 , from RHIC to LHC approximately doubles both the GLV and BDMS energy loss.

In distinction to pQCD, the stopping distance for light quark jets in the falling string holographic scenario was found in [29] to be bounded by $L_T < \kappa E^{1/3}/T^{4/3}$. This can be simulated via Eq. (5) by choosing $a > (2-b)/3$ in the range $a \in [0, 1/3]$. The special case $b = 2$ and $a = 1/3$ is the one favored phenomenologically [76–78, 82] by the high p_T azimuthal anisotropy $v_2(p_T)$ data. For that case, $dE_{AdS}/dL = -\kappa E^{1/3} L^2 T^{11/3}$. Thus the energy loss grows even faster with density, $\propto \rho^{11/9}$. We see that quite generally dE/dL should increase significantly with density.

For a more realistic Bjorken longitudinally expanding plasma of transverse thickness L the density decreases approximately as $T^3(\tau) \propto (dN_{ch}/dy)/(\tau L^2)$. In this Bjorken brick case

$$\frac{P(L)}{P(0)} = \left(1 - \kappa' \frac{(dN/dy)^{(2-a+b)/3}}{(LP(0))^{1-a}} \right)^{\frac{1}{1-a}}. \quad (6)$$

To estimate the variation of R_{AA} in this case consider the distribution of initial jet transverse momenta (at mid rapidity) approximated as

$$d\sigma(p_T)/dp_T \propto 1/p_T^{n(p_T, s)} \quad (7)$$

with $n(p_T, s) \equiv -d \log(d\sigma(s))/d \log(p_T)$ given by the cm energy dependent parton spectral index computed from pQCD.

The nuclear modification factor for jet partons (neglecting hadron fragmentation) is simply a change of variables which leads with Eq. (6) for a fixed centrality class

to

$$R_{AA}(p_f; s, A) = \frac{\partial p_0}{\partial p_f} \frac{d\sigma(p_0(p_f))/dp}{d\sigma(p_f)/dp} \approx \left(1 + \kappa' \frac{(dN/dy)^{(2-a+b)/3}}{(Lp_f)^{1-a}} \right)^{\frac{a-n(p_f)}{1-a}}. \quad (8)$$

Given a model specified by (a, b) the coupling parameter $\kappa'(a, b)$ can be fixed by fitting RHIC R_{AA} at one reference momentum, e.g. $p_T = 10$ GeV/c.

We show in Fig. 2 the evolution of this simple analytic model of R_{AA} from RHIC to LHC for the case $a = 1/3$ energy loss and for different $b = 0, 1, 2$ that correspond to path length scaling for elastic, inelastic and AdS falling strings scenarios. For this qualitative plot, we take spectral indices (see Fig. 3 of the next section) as $n_{RHIC} \equiv n_1(p_T) \approx 5.5 + (p_T - 10)/10$ that rises by 1 unit in the $p_T = 10 - 20$ range at RHIC 0.2 ATeV, while $n_{LHC} \equiv n_2 \approx 4.5$ approximately independent of p_T at LHC 2.76 ATeV. We fix κ' for each b by demanding $R_{AA}(p_T = 10, dN/dy = 1000) = 0.2$. The RHIC blue curve is therefore independent of the b parameter. For larger a the blue curve flattens, while for smaller a the curve rises with p_T more rapidly. The $a = 1/3$ rise is within the large error band of the PHENIX data shown in Fig. 1.

It is important to note that if there were no density dependence of energy loss, then just because the spectral index decreases from ~ 5.5 to 4.5, the $R_{AA}(LHC)$ would be less quenched by $\sim 70\%$ at $p_T = 10$ GeV/c at LHC! However, the approximate doubling of the initial density (and hence dE/dL) at LHC relative to RHIC results in halving R_{AA} at $p_T = 10$ GeV/c relative to RHIC. In addition, the reduction of the fractional energy loss with increasing p_T with $a = 1/3$ causes R_{AA} to rise with p_T at LHC while at RHIC the p_T dependent increase of the spectral index compensates this natural rise. We will confirm these generic features in the next section with detailed WHDG numerical calculations.

With this simple analytic model we can also easily explore the sensitivity of the LHC extrapolation to the path length dependence parameter b . The b parameter influences mainly the scaling exponent of dN/dy in the Bjorken expanding case. We see that decreasing b to 0 (simulating perturbative elastic energy loss) decreases the difference between RHIC and LHC at $p_T = 10$ GeV/c but the change in p_T slope is similar. For $b = 2$ (simulating an L^3 path dependence suggested by AdS falling strings) predicts a significantly larger density dependence from RHIC to LHC. The cross over momentum where R_{AA} at RHIC and LHC are equal increases monotonically with b . The absolute value of R_{AA} and its p_T slope therefore provide strong constraints on the a, b parameters and therefore on the initial density or dN/dy dependence, $\rho^{(2-a+b)/3}$. None of the parametric models predicts similar nuclear modification factors at RHIC and LHC above $p_T > 10$ GeV/c.

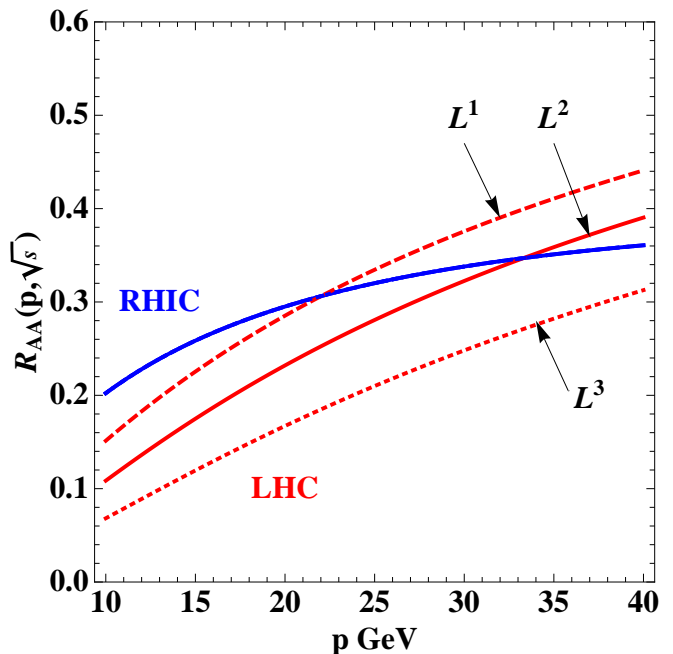


FIG. 2. Schematic nuclear modification factor model Eq. (8) for a “Bjorken plasma brick” normalized to $R_{AA}(p_T = 10) = 0.2$ for central RHIC (blue) assuming $a = 1/3$. The momentum dependence at RHIC is independent of b once the reference normalization at $p_T = 10$ GeV/c is fixed. The red curves for LHC are evaluated with initial rapidity density scaled up by a factor 2.0 relative to RHIC. The $b = 0, 1, 2$ dependent extrapolations to LHC (red dashed, solid, dotted) are labeled by the equivalent L^b path length dependence of the total energy loss in the static plasma limit.

III. JET TOMOGRAPHY: QUANTITATIVE

The extraction of tomographic (density dependent) information from R_{AA} , and suppression observables in general, is complicated by many competing physics processes—some of which are interesting in their own right. Of greatest import for our discussion is the initial phase space distribution of high- p_T quarks and gluons in both coordinate and momentum space. At RHIC, extensive reference spectra from p + p collisions at the same \sqrt{s} as in Au + Au collisions allow for a precise calibration of R_{AA} and constrain experimentally the initial quark and gluon spectra. The control d + Au data were essential to calibrate the magnitude of the initial state nuclear distortions of the initial jet spectra due to gluon saturation/shadowing physics [11, 61, 67, 83, 84]. At midrapidity the initial high- p_T partonic spectrum in the $(x, Q^2) \sim (0.1, 100) - (0.2, 400)$ kinematic range was not found to deviate significantly from the reference p + p pdfs (see Fig. 1 of [84]). Direct photon measurements further confirmed that the binary collision scaling based on Glauber diffuse nuclear reaction geometry can be used to understand the nuclear number and impact parameter dependence of hard processes [85].

Comparable control measurements do not yet exist at LHC, thereby severely limiting the strength of conclusions that can be drawn from the first R_{AA} data [1]. The absence of reference $p + p$ data leads alone to about a factor ~ 2 , p_T -dependent systematic uncertainty in the normalization of the reported R_{AA} . This uncertainty is shown for the 0-5% centrality data by the yellow band in Fig. 1. Second, the absence of control $p + \text{Pb}$ as yet makes it impossible to deconvolute *initial state* nuclear suppression of high- p_T particles due to small x gluon saturation, or Color Glass Condensate (CGC) [11, 62–68], effects at LHC in the $Q^2 > 100 \text{ GeV}^2$ range. Because the fractional momenta relevant for midrapidity jet production at LHC are 10 times smaller at a given p_T than at RHIC strong initial state suppression of the nuclear/gluon structure has been predicted in [68] at LHC.

In this work, we assume the absence of significant initial-state suppression in the $p_T \sim 10 - 20 \text{ GeV}/c$ kinematic region corresponding to $(x, Q^2) \sim (0.01 - 0.02, 100 - 400 \text{ GeV}^2)$. This is consistent with the DGLAP Q^2 evolution of global fits to nuclear pdfs (see Fig.1 of [84]). The first ATLAS measurement [86] of Z boson candidates is also consistent with unshadowed binary scaling of jets in the $x \sim 0.05$ kinematic range. Future direct photon measurements at LHC will provide additional control over initial state shadowing/CGC effects.

The new ALICE data show features that appear strikingly similar to expectations based on pQCD energy loss: in particular R_{AA} rises significantly at LHC as a function of p_T rather than the observed flatness within errors at RHIC. In [46] the predicted stronger rise as a function of momentum at LHC can be understood from the qualitative model in Section II and the also from the following even simpler schematic model: The fractional energy loss of a high- p_T parton decreases in pQCD with momentum as $\epsilon \sim \log(p_T)/p_T$. The final momentum, p_T^f , is related to the initial momentum, p_T^i , by $p_T^f = (1 - \epsilon)p_T^i$. For particle production distributions approximated by a power law, $dN/dp_T \sim p_T^{-n}$, the nuclear modification factor $R_{AA} \sim \langle (1 - \epsilon)^{n-1} \rangle$. The suppression at RHIC is flatter than at LHC due to an accidental cancellation between 1) the fraction of high- p_T gluons to quarks (see the upper panel of Fig. 3), 2) the hardening of the production spectrum as a function of p_T (see the lower panel of Fig. 3), and 3) the decrease in energy loss as a function of p_T (see Fig. 4).

As shown in the lower panel of Fig. 3 at LHC, the production spectrum is much harder (smaller \sim constant spectral index) than at RHIC. For a constant $n(p_T)$ the decrease of fractional energy loss with p_T would lead to an R_{AA} that increases with p_T . One can see from Fig. 1 that the WHDG prediction rises with p_T similar to the ALICE data.

As one can see from the top panel of Fig. 3, also in contrast to RHIC, LO pQCD predicts that hard jets at LHC are predominately gluons to much higher p_T . Naïvely then, with larger density, larger medium size (for Pb vs.

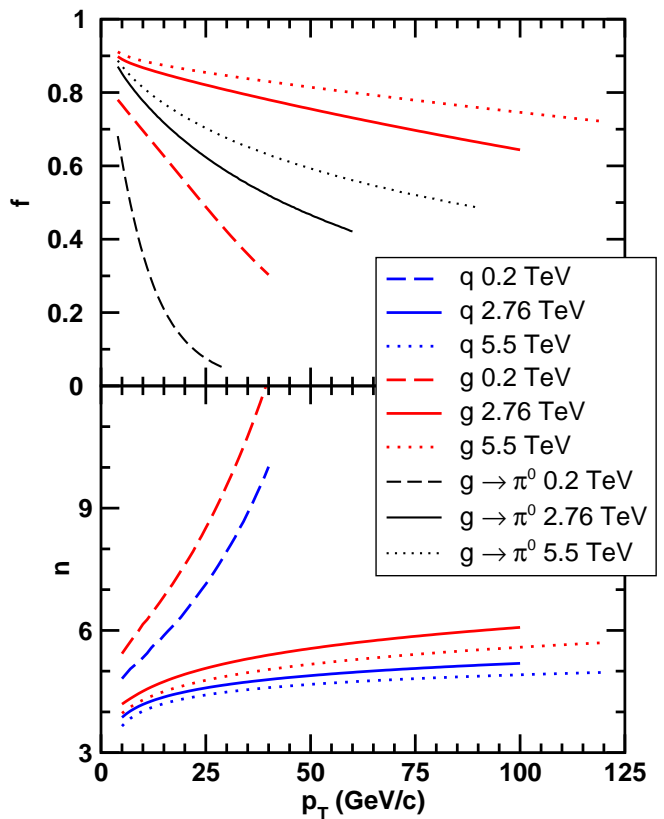


FIG. 3. (Top) Fraction of jets that are gluons as a function of jet p_T from LO pQCD [87] for $\sqrt{s} = 0.2, 2.76,$ and 5.5 TeV shown in red. Black curves show fraction of pions fragmenting from gluons at final pion p_T . (Bottom) Partonic spectral index, $n(p_T) = -d \log(dN/dy dp_T)/d \log(p_T)$, of initial $y = 0$ gluon (red) and light quark (blue) jets compared at RHIC and LHC in $p + p$.

Au), and the greater preponderance of gluons with 9/4 enhanced energy loss relative to quark jets, should lead to an R_{AA} suppressed much below that seen at RHIC. However, the smaller and flatter spectral indices of both quarks and gluons compensates in the other direction.

The first numerical GLV prediction for $R_{AA}^{\pi^0}$ in 2002 for 5.5 ATeV Pb + Pb collisions LHC including only radiative energy loss was given in Fig. 3 of [46] and overlaps well with the yellow ALICE systematic error band in Fig. 1. The first predicted WHDG R_{AA} for LHC (see Fig. 83 of [71]) including elastic energy loss as well as radiative energy loss and also realistic geometric jet path fluctuations accidentally remained close to Vitev’s original GLV prediction. Our currently updated WHDG study incorporates the observed 2.2 times increase in charged particle rapidity density by ALICE in Pb+Pb 2.76 ATeV collisions to extrapolate the most recent $1 - \sigma$ uncertainty band of initial sQGP densities compared to high statistics PHENIX data from RHIC: this is the blue band in Fig. 1, which shows a significant underprediction of the ALICE data.

We discuss in more detail below a range of theoretic-

cal and experimental issues that need further attention as jet tomography advances toward a more quantitative level. The RHIC constrained WHDG results for R_{AA} appear consistent with the ALICE data and the earlier estimates within the present very large error band due to the unknown p + p baseline at this energy. While stronger conclusions are not warranted at this time, perturbative QCD tomography is at least consistent with the striking positive slope p_T dependence of the nuclear modification light parton jet fragments at LHC. The change of the p_T slope, dR_{AA}/dp_T , from negative at SPS to approximately zero at RHIC and finally to positive at LHC is a critical consistency test for the pQCD framework that jet holographic approaches must (eventually) also be able to pass.

IV. FROM ENERGY LOSS TO R_{AA}

A. 0-5% Central

The WHDG energy loss calculation described in [53, 88] uses the first order in opacity radiative energy loss and Braaten-Thoma pQCD collisional partonic energy loss. The model assumes Debye-screened color scattering centers, and one loop screening mass $\mu = gT$. Both light quarks and gluons have one loop medium-induced thermal masses of order μ . As noted previously, a generic feature of this pQCD radiative energy loss is that the fraction of final momentum to initial momentum of the parent parton, $\epsilon = p_T^f/p_T^i$, scales as $\epsilon \sim \log(p_T)/p_T$ as can be seen Fig. 4. Of crucial importance in this formalism is the quantum interference between the hard vacuum radiation due to the initial creation of a hard parton and the radiation induced by scatterings in the medium.

The redistribution of energy via collisional processes is found through the use of the fluctuation-dissipation theorem with the mean loss given by the thermal field theory calculation of Braaten and Thoma[89]. This redistribution of energy can lead to the high- p_T parton either losing or gaining energy, which is taken into account. The simple Gaussian approximation due to the fluctuation-dissipation theorem is a simplification that future more detailed but unwieldy elastic energy loss calculations can improve [90]. One can see in Fig. 4 that, with these assumptions and at medium densities appropriate for RHIC and LHC, at moderate $p_T \lesssim 20$ GeV elastic energy loss is as important as inelastic at both RHIC and LHC.

We note in passing that the production points of the high momentum particles are distributed according to the binary distribution T_{AA} ; the medium density is assumed proportional to the participant density given by the Glauber model, and 1-D Bjorken-expansion is approximately included by evaluating the density at a time one half the path length.

R_{AA} is defined as the ratio of observed spectra in A + A collisions for a given centrality divided by the observed spectrum in p + p collisions scaled by the number of

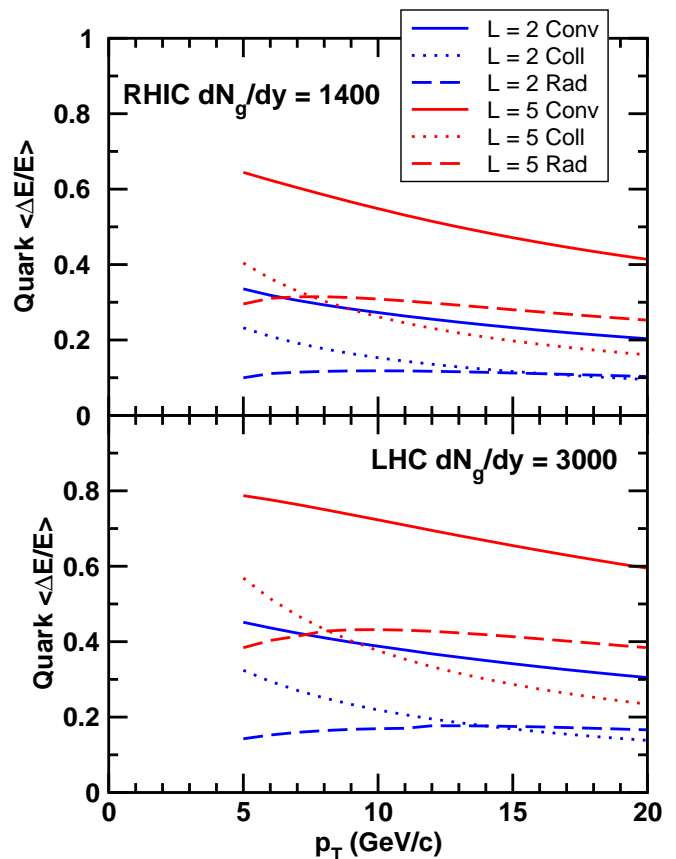


FIG. 4. Average fractional energy loss $\langle \epsilon \rangle = \langle \Delta E/E \rangle$ for a light quark of initial momentum p_T in a Bjorken-expanding brick of plasma of length 2 fm (blue) and 5 fm (red) for RHIC (top) and LHC (bottom) conditions from the WHDG energy loss model [53]. $\langle \epsilon \rangle$ is shown for purely radiative energy loss (Rad), purely collisional energy loss (Coll), and the incoherent convolution of the two (Conv). Elastic energy loss is a crucial contribution to total energy loss at both RHIC and LHC.

binary collisions at the given centrality. ALICE measured the R_{AA} of hadrons using the non-invariant spectra,

$$R_{AA}^{h^+h^-}(p_T, b) = \frac{dN_{AA}^{h^+h^-}/dp_T dy}{N_{\text{coll}}(b) dN_{pp}^{h^+h^-}/dp_T dy}, \quad (9)$$

When one assumes that the production points of hard particles is proportional to the T_{AA} distribution, where $N_{\text{coll}} = \int d^2\mathbf{x} T_{AA}(\mathbf{x})$, N_{coll} drops out of the theoretical calculation. However it is important to note that the values of N_{coll} that we find using the optical Glauber model with the same parameters listed in [1] significantly disagree with those used by ALICE, found using a Monte-Carlo approach; we quantify this discrepancy in Table I. We will come back to this difference when we discuss R_{cp} below.

In order to make contact with the experimentally observed hadrons, the partonic energy loss described above must be convolved with a partonic production spectrum and a set of fragmentation func-

Cent.	ALICE N_{coll}	ALICE Rel. Unc.	Opt. Gl. N_{coll}	% Diff
0-5%	1690 ± 131	$\sim 8\%$	1710	$\sim 1\%$
70-80%	15.7 ± 0.7	$\sim 5\%$	12.6	$\sim 25\%$

TABLE I. Values of N_{coll} used by ALICE and those found using an optical Glauber model with a Woods-Saxon geometry and inelastic cross section identical to those used by ALICE in their Monte-Carlo calculation. Cf. to the uncertainties shown in Fig. 6.

tions (FFs). We compute partonic suppressions via $R_{\text{AA}}^{q,g} = \langle (1 - \epsilon(\mathbf{x}, \phi))^{n^{q,g}(p_T)^{-1}} \rangle$, where we take $n^{q,g} = d \log(dN^{q,g}/dp_T)/d \log(p_T)$ to approximate the power law for the partonic production spectrum, and $\langle \dots \rangle$ represents an averaging over the geometry for a given centrality class. Then

$$R_{\text{AA}}^h(p_T; b) = \int \frac{dz}{z} \frac{dN^q}{dp_T} \left(\frac{p_T}{z} \right) R_{\text{AA}}^q \left(\frac{p_T}{z}; b \right) D^{q \rightarrow h}(z) + q \rightarrow g / \int \frac{dz}{z} \frac{dN^q}{dp_T} \left(\frac{p_T}{z} \right) D^{q \rightarrow h}(z) + q \rightarrow g \quad (10)$$

We use a LO pQCD code [87] with a K factor of 3, CTEQ5L parton distribution functions [91] evaluated at $Q = p_T/2$, and KKP fragmentation functions [92]. It is important to emphasize that the factor of two systematic uncertainty in the K factor drops out of the ratio above. The produced neutral pion spectra expected for p + p collisions at RHIC and LHC energies using this LO pQCD procedure are shown in the top panel of Fig. 5. The LO pQCD spectrum at $\sqrt{s} = 0.2$ TeV agrees well with the PHENIX data to within $\pm 20\%$. On the other hand we find that our LO pQCD spectrum with $K = 3$ evaluated at $\sqrt{s} = 2.76$ TeV systematically overpredicts the spectrum used by ALICE by a nearly p_T -independent factor of ~ 2 . We will come back to the absolute cross section normalization differences below.

One of the key ingredients in an energy loss calculation is the density of the medium through which a fast parton propagates. We assume the transverse coordinate dependence of the density of the quark-gluon plasma medium is proportional to the participant density, $dN_g/d^2\mathbf{x}dy \propto \rho_{\text{part}}$. The proportionality constant that connects these two quantities is precisely the lowest order tomographic information we can deduce by comparing energy loss calculations with data. The PHENIX collaboration extracted this constant, reported as dN_g/dy , via a rigorous statistical analysis comparing the WHDG energy loss to the 0-5% central RHIC $R_{\text{AA}}^{\pi^0}(p_T)$ data [34]; it was found that the best fit value and one standard deviation uncertainty are $dN_g/dy = 1400_{-375}^{+200}$ for a fixed $\alpha_s = 0.3$. Once this constant is fixed and we make the assumption that the quark-gluon plasma medium density scales with the observed number of charged hadrons, the QGP medium density at LHC is predicted. ALICE reported

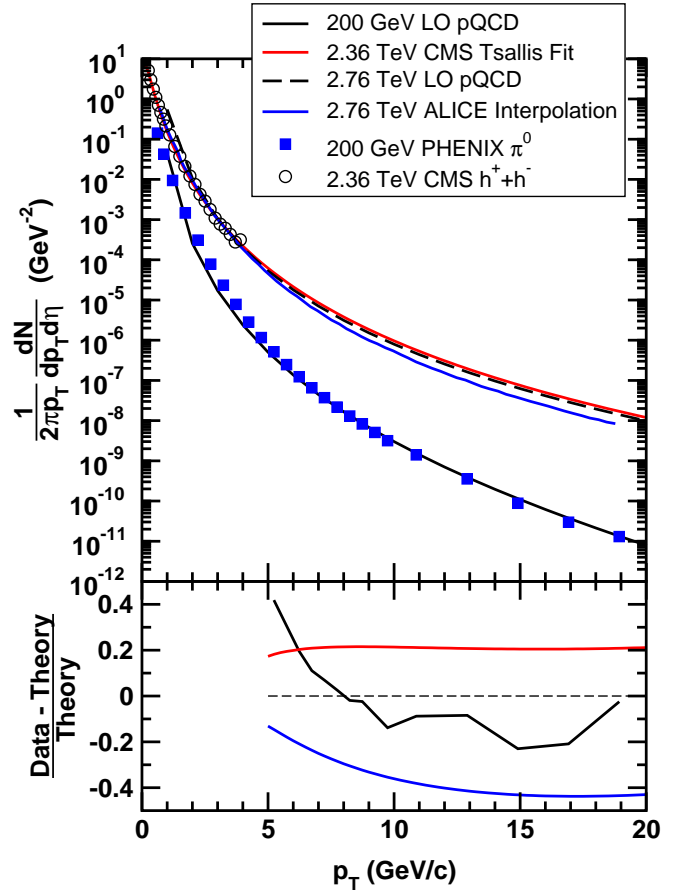


FIG. 5. (Top) Hadron production spectrum data in p + p collisions from PHENIX at $\sqrt{s} = 0.2$ TeV [93] and from CMS at $\sqrt{s} = 2.36$ TeV [94]; the Tsallis distribution that is a best fit to the low p_T CMS data is shown in red. Also in the figure is the LO pQCD calculation at $\sqrt{s} = 0.2$ TeV (black) and $\sqrt{s} = 2.76$ TeV (dashed black). The interpolation spectrum used by ALICE to normalize R_{AA} at $\sqrt{s} = 2.76$ TeV is shown in blue. (Bottom) The PHENIX data normalized to $\sqrt{s} = 0.2$ TeV LO pQCD (black), the CMS Tsallis fit at $\sqrt{s} = 2.36$ TeV normalized to LO pQCD at $\sqrt{s} = 2.76$ TeV (red), and the ALICE interpolation normalized to LO pQCD at $\sqrt{s} = 2.76$ TeV (blue). Despite a larger \sqrt{s} , note that the ALICE interpolation is a factor $\gtrsim 2$ smaller than the CMS Tsallis fit, emphasizing the obvious need for 2.76 pp reference data.

that the 0-5% central value of $(dN_{\text{ch}}/d\eta)/(N_{\text{part}}/2)$ increased by a factor of 2.2 from RHIC [2]; the scaled density in 0-5% central collisions at $\sqrt{s_{\text{NN}}} = 2.76$ TeV is then $dN_g/dy = 3000_{-800}^{+500}$.

With the QGP medium density at LHC so fixed, the suppression from the WHDG model is a *constrained prediction*; i.e. there are no free parameters in our calculation. We compare the resulting suppression for 0-5% central $R_{\text{AA}}^{\pi^0}(p_T)$ in Fig. 1 to the 0-5% central ALICE charged hadron suppression. The results from the one standard deviation uncertainty in dN_g/dy are represented by thin blue lines; a light blue shaded region connects the two, denoting the uncertainty in the the-

oretical calculation due to the uncertainty of the extracted medium parameter from RHIC data. The dashed blue line represents $R_{AA}^{\pi^0}(p_T)$ for the best fit value of $dN_g/dy = 3000$. One can see from the figure that the perturbative calculation qualitatively describes the increase in R_{AA} as a function of p_T , as we expected. Also our pocket formula from above describes the low- p_T normalization of the WHDG R_{AA} results rather well. The small, $\lesssim 0.1$ value of R_{AA} at low- p_T demonstrates again that the WHDG energy loss model is not fragile. The realistic distribution of production points and medium density means there is no (appreciable) corona of jets that emerge unmodified; there is no lower bound to the theoretical value of R_{AA} .

On the other hand, the very low normalization of the WHDG R_{AA} seriously underpredicts the central values of the ALICE data. As there is no measured p + p baseline at $\sqrt{s} = 2.76$ TeV at LHC yet, ALICE reports a very large uncertainty in R_{AA} due to the uncertainty in the interpolated p + p baseline used. The result is that the 0-5% central WHDG energy loss calculation and the ALICE data agree at the edge of their respective reported 1- σ uncertainties. It is worth emphasizing again, that while the WHDG R_{AA} prediction is independent of the normalization of the p+p reference, the ALICE R_{AA} is sensitive to the unmeasured p+p reference that has an intrinsic theoretical factor of \sim two systematic uncertainty at both LO and NLO level.

In addition to the theoretical uncertainty due to the finite precision extraction of a medium density at RHIC, there are also systematic uncertainties in the theoretical calculation due to simplifying approximations made in the derivation of energy loss formulae. Some of these uncertainties have been quantified [95], and it turns out that the uncertainty due to the collinear approximation is in fact quite large: an exploration of this systematic theoretical uncertainty yields a factor of 3 uncertainty in the extracted medium density at RHIC when energy loss is assumed to be radiative only. Given this large uncertainty, one might naïvely expect a similarly large uncertainty in the WHDG predictions for R_{AA} at LHC. However this expectation is incorrect for two reasons: first, the uncertainty due to the collinear approximation decreases significantly when elastic energy loss is included [95]. Second, observables such as $v_2(p_T)$ —once the reference opacity is fixed—are found numerically not to depend much on the specifics of the explored collinear approximation uncertainty [96]. The theoretical systematic uncertainties of the elastic energy loss contributions are less well known and call for more scrutiny. In [90] it was shown that, contrary to often assumed multi soft Gaussian transverse elastic diffusion approximation, the large momentum transfer power law tails with $q \sim 10T \sim 2$ GeV momentum exchange (as included in WHDG through the $\log(E/T)$ enhancement of elastic energy loss), cannot be ignored as assumed in many other models. In order to quantify the size of this collinear radiation approximation systematic uncertainty we use the

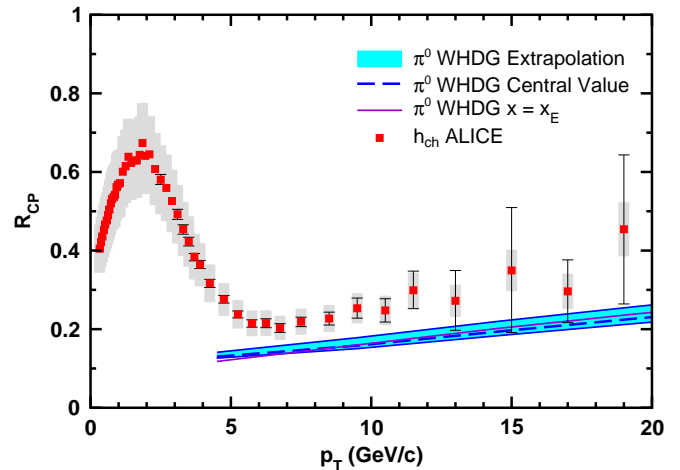


FIG. 6. R_{cp} , the ratio of 0-5% central $R_{AA}(p_T)$ to 70-80% peripheral $R_{AA}(p_T)$, from ALICE and our WHDG calculations. Experimental errors were added in quadrature, with those uncertainties due to the unknown p + p baseline cancelled.

inelastic energy loss formula derived in Minkowski coordinates and take the maximum angle of emission for radiation to be $\theta_{\max} = \pi/2$ (for a more detailed discussion, see [95]). The best fit value for the average medium density constrained by central RHIC data is $dN_g/dy = 1400$ [95], which extrapolates to $dN_g/dy = 2800$. The purple curves in Fig. 1 and denoted by “ $x = x_E$ ” in Fig. 6 shows the values of $R_{AA}(p_T)$ that result. That the curve lies within the WHDG uncertainty blue band due to the 1- σ medium parameter extraction at RHIC confirms that the systematic theoretical uncertainty due to the collinear approximation is small for R_{AA} at LHC once the medium parameter is fixed to RHIC data; in particular, the WHDG predictions and the ALICE data are in quantitative tension within the combined experimental and currently quantitatively explored theoretical uncertainties.

B. 70-80% Peripheral and R_{cp}

Continuing with the assumption that the QGP medium density scales with the number of charged hadrons we may make another *constrained prediction* from WHDG for the R_{AA} of the 70-80% centrality class. From the ALICE centrality-dependent multiplicity data [4] we find that $dN_g/dy(70 - 80\%) = 66_{-17}^{+10}$, and $dN_g/dy = 62$ for the $x = x_E$ calculation. These are admittedly very small densities distributed over a small region, and it is not clear that a QGP medium forms in these highly peripheral heavy ion collisions. Nevertheless we have assumed that our energy loss formalism is valid in both deconfined and confined media; it is not unreasonable to compare our results to the data, and our calculation and the ALICE results shown in Fig. 1.

Since there is so much uncertainty in the p + p baseline spectrum, we find it useful to examine R_{cp} , which is the

ratio of central R_{AA} to peripheral R_{AA} , in this case

$$R_{cp}(p_T) = \frac{R_{AA}(p_T; 0 - 5\%)}{R_{AA}(p_T; 70 - 80\%)}. \quad (11)$$

We plot both the experimental values and our calculation in Fig. 6. Care was taken to propagate the relative systematic and statistical errors in quadrature. Some component of the systematic uncertainty shown in the original ALICE figures [1] is due to a p_T -dependent uncertainty from the unknown p + p reference spectrum, which cancels in the R_{cp} ratio. The ALICE paper [1] quotes the systematic uncertainties not due to the p + p spectrum as 5-7% and 8-10% in the central and peripheral bins, respectively. As a conservative estimate we take the upper values and add (in quadrature) the relative uncertainty due to the N_{coll} normalization; this procedure yields a systematic uncertainty of 15%, represented by the gray bands in Fig. 6. Again the light blue band represents the theoretical uncertainty due to the extraction of the medium density at RHIC, with the dashed blue curve representing the best fit value, and the thin purple curve represents the result when using the $x = x_E$ calculation discussed above.

The theoretical calculation reproduces the observed p_T -dependence of R_{cp} quite well. The theory results are systematically about 2 standard deviations of systematic uncertainty below the data; however one should note that much of this systematic error is correlated and p_T -independent, and a smaller peripheral N_{coll} , as suggested by the results from an optical Glauber calculation, would yield an experimental R_{cp} suppression significantly closer to our prediction. Precise observations of direct photons and Z bosons should help reduce this possible extra uncertainty on the number of binary collisions in highly peripheral events. Additionally, that the optical Glauber results deviate so significantly from the Monte Carlo results in the 70-80% centrality bin provides a quantitative feel for the importance of geometry fluctuations for these highly peripheral collisions; these possibly large geometry fluctuations are not taken into account in the energy loss calculations presented here. Nevertheless, we find that this large discrepancy is a challenge to the pQCD paradigm assumed by the WHDG energy loss calculation.

In Fig. 7 we present our predictions for $R_{AA}^{\pi^0}$ measured in Pb + Pb collisions at 2.76 at LHC out to $p_T = 40$ GeV/c. Fig. 8 shows our predictions for central and peripheral suppression of neutral pions at $\sqrt{s_{NN}} = 5.5$ TeV. Assuming that charged particle multiplicity scales as $(s_{NN})^{0.15}$, as ALICE reported by fitting current world data [2], and assuming medium density scales with the observed charged particle multiplicity, we have that at $\sqrt{s_{NN}} = 5.5$ TeV the extrapolation from the RHIC extraction is $dN_g/dy = 3700_{-1000}^{+500}$; the light blue band in the figure represents the predicted suppression based on these medium densities, with the dashed blue curve representing the most likely value. The thin purple curve represents the result when using the $x = x_E$ prescription and an extrapolation of $dN_g/dy = 3500$. We note that

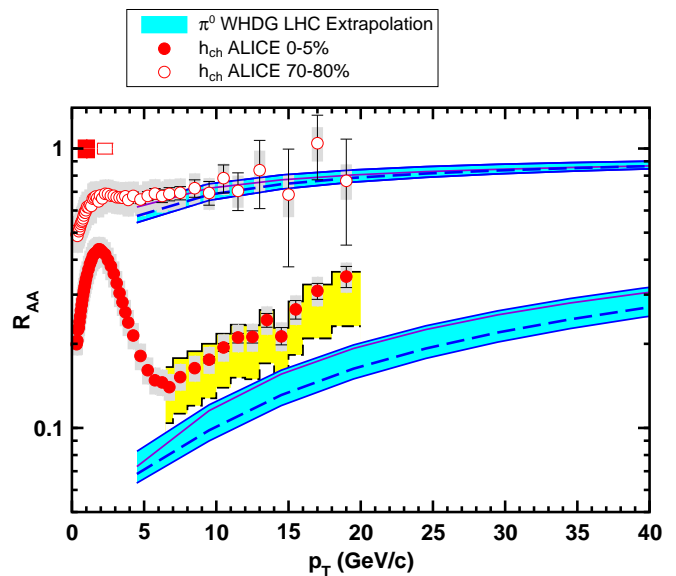


FIG. 7. Predictions of $R_{AA}^{\pi^0}$ for Pb + Pb collisions at 2.76 ATeV from the WHDG energy loss model out to $p_T = 40$ GeV/c compared to current ALICE measurements of $R_{AA}^{h_{ch}}$ [1].

these constrained predictions for 5.5 ATeV are qualitatively similar but differ in detail from our earlier 2007 predictions that assumed a smaller medium density range, $dN_g/dy = 1700 - 2900$ [72]. These updated WHDG constrained predictions are qualitatively similar also to the predictions from 2002 GLV [46] that assumed smaller opacities at 5.5 ATeV but neglected the competing effects due to elastic and radiative energy loss as well as path length fluctuations included in WHDG. Similar perturbative overquenching was also noted in other energy loss model approximations in [70, 97, 98]. As emphasized in Section II overquenching is a generic robust prediction of density dependent dE/dL models.

V. CONCLUSIONS AND DISCUSSION

In this paper we compared $\pi^0 R_{AA}(p_T)$ and $R_{cp}(p_T)$ from the WHDG energy loss model [53] at $\sqrt{s_{NN}} = 2.76$ TeV and the recent ALICE data on charged hadron suppression at LHC [1]. The WHDG model includes both radiative and collisional channels and jet path length fluctuations. We found that at the momentum range currently probed at LHC, collisional energy loss is as important as radiative energy loss and cannot be neglected. Previous work [99] showed that even at top LHC energies and $p_T \sim 250$ GeV, elastic energy loss makes up a sizable fraction, $\sim 25\%$, of the total energy loss in the HTL pQCD picture of the sQGP. The results we present assume that the HTL QGP medium density scales with the global charged particle multiplicity. Our results are true predictions based on rigorous statistical constraints of the medium density using WHDG at RHIC to the

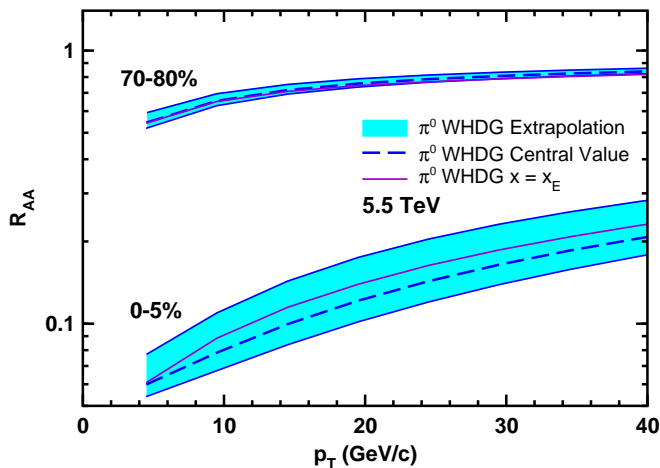


FIG. 8. Central and peripheral $R_{AA}^{\pi^0}$ at $\sqrt{s_{NN}} = 5.5$ TeV from the WHDG energy loss model.

QGP conditions at 2.76 central Pb+Pb as constrained by global dN_{ch}/dy from ALICE: *there are no free parameters*. While unconstrained models without elastic energy and path length fluctuations can fit any R_{AA} by adjusting the opacity, consistency with extensive RHIC jet quenching data leads in WHDG to a prediction of overquenching relative to the first ALICE R_{AA} data.

We find that our results show a qualitative agreement with the momentum dependence of the central ALICE data and a quantitative agreement with the normalization and p_T -dependence of the peripheral ALICE results, within the reported uncertainties. Under our assumption of the scaling of the medium density, though, we find a quantitative disagreement with the normalization of the suppression for the reported central values of the ALICE data for 0-5% central Pb + Pb collisions. Unfortunately, the very large systematic uncertainty in the ALICE data due to the unmeasured base p + p reference precludes strong conclusions at this time. Our calculated R_{AA} is free from this normalization ambiguity, but the experimental systematic error is dominated by it, and our predictions for central R_{AA} are not in disagreement with the data within this large systematic uncertainty. Only a p + p run at $\sqrt{s} = 2.76$ TeV at LHC will resolve this uncertainty.

In order to reduce systematic uncertainties, we therefore compared R_{cp} within the WHDG framework. An R_{cp} analysis from ALICE was not released yet, and therefore we calculated this quantity from the available results including propagating the reported uncertainties.

The WHDG results for R_{cp} also show qualitative agreement with the p_T -dependent shape of the data, although the WHDG calculations seem to somewhat under-predict the slope for the central and peripheral $R_{AA}(p_T)$ individually. On the other hand, since our central R_{AA} calculations are more suppressed than the R_{AA} data while the peripheral results compare favorably, our R_{cp} results also over-suppress the R_{cp} data. This disagreement is

at about the $2\text{-}\sigma$ level compared to the 15% systematic error we estimate from the ALICE data. Much of the 15% systematic uncertainty is due to the N_{coll} normalization of R_{AA} and is therefore p_T -independent and correlated, reducing the tension between the experimental results and the theoretical predictions. It is also worth noting again that the N_{coll} used by ALICE differs significantly from that given by an optical Glauber calculation. Our results would compare more favorably with the data if the optical Glauber N_{coll} calculation would be used. Precise experimental measurements of high- p_T probes that interact only weakly with the QGP plasma, such as direct photons or Z bosons, is the only way of experimentally constraining the N_{coll} normalization used in R_{AA} and R_{cp} analyses. Z bosons will give a much cleaner picture as photons are created not only directly in the initial hard scatterings but also via photon bremsstrahlung [100–102].

As hard photons and Z bosons come from quark-antiquark annihilation, a measurement of R_{AA}^γ or R_{AA}^Z less than 1 could be interpreted as due to either a reduction in the expected number of binary collisions or the reduction in the availability of anti-quarks due to gluon saturation. In particular there are predictions of a reduction by $\sim 50\%$ in the initial hard spectra at the momenta currently observed at LHC due to gluon saturation effects [68]; this reduction would naturally decrease as a function of p_T as x increases. As such, the p_T -dependence of the ALICE data may be due, at least in part, to initial state effects. A precise measurement of R_{AA}^γ or R_{AA}^Z showing the p_T -independence of these ratios would be required to demonstrate the lack of strong initial state shadowing in the $x > 0.01$ and $Q^2 > 100$ GeV² range relevant to the present ALICE data in the $p_T = 10 - 20$ GeV range (as expected from, e.g., [84]). p + A collisions would provide a superb independent test of the possible influence of gluon saturation, similar to the crucial d + A collisions needed at RHIC to disentangle initial state from final state effects.

Since there are no adjustable parameters for us, the significant tension between our results and the ALICE data is a failure to *simultaneously* describe the normalizations of both the RHIC and LHC $R_{AA}(p_T)$. One possibility is the sQGP produced at LHC is in fact more transparent than predicted by perturbative QCD tomographic models with medium densities that scale with observed particle rapidity densities.

Theoretical possibilities that could contribute to the apparent transparency (decreased opacity) of the sQGP relative to the WHDG extrapolation from RHIC to LHC include

1. Baryon anomaly [103–105]
2. Gluon feedback [106]
3. Gluon to quark jet conversion [101]
4. Gluon self energy [48, 49]

5. Is the jet-medium coupling reduced at LHC:
 $\alpha_s(LHC) < \alpha_s(RHIC)$?

Item 1 can be resolved when identified $\pi, K, p, \Lambda, \dots, \Omega^-$ high- p_T R_{AA} becomes available. Item 2, in which the bremsstrahlung emitted gluons are kept track of and produce observed hadrons, may be a partial explanation, but estimates so far have neglected the energy loss of the radiated gluons themselves. Radiated gluons with formation length less than the size of the medium could also be strongly quenched. A detailed centrality dependence of the di-hadron correlations may be able to resolve such nonlinear gluon shower feedback mechanisms. Item 3 is possible channel that can effectively reduce the gluon jet color charge for asymmetric ($|x - 0.5| \sim 0.5$) $q\bar{q}$ conversion. However, estimates[101] so far have neglected strong interference effects of medium and vacuum induced amplitudes in finite size plasmas and high p_T octet color coherence of pair production. Jet flavor triggers that could discriminate light quark and gluon jets are needed to determine experimentally if this mechanism is responsible for the apparent transparency of the sQGP at LHC. Item 4 involves HTL gluon dispersion effects on both the induced and hard initial radiation associated with jet production. In [48, 49] it was shown that the Ter-Mikayelian and transition radiation effects reduce in general the effective dE/dL . Comparison of the centrality (or path length L) dependence of R_{AA} may help untangle such dispersion effects.

Item 5 refers to the possibility that the surprisingly transparent sQGP at RHIC could be due a reduction of the effective jet-medium coupling between RHIC and LHC. In the WHDG analysis here, we assumed $\alpha = 0.3$ is the same at RHIC and LHC and the R_{AA} difference only reflects the increase of the initial sQGP density by 2.2. In [70] an average path length approximation using GLV [42, 43] was used to show that approximately the same effective opacity $L/\lambda \approx 6$ can fit both RHIC and LHC R_{AA} . In the HTL approximation $1/\lambda \propto T/\alpha^2$ up to slowly varying logarithmic corrections, so at L/λ constant implies α is reduced by a factor of $2.2^{1/3} = 1.3$. However, in [70] $\alpha_s = 0.3$ was assumed to be constant and L varied. In WHDG the effective L is completely fixed the distribution of path lengths. As $\Delta E_{rad} \propto \alpha_s^3$ and $\Delta E_{el} \propto \alpha_s^2$ the theoretical calculation of suppression depends very strongly on the specific value of α_s taken. A fit, i.e. a postdiction to the LHC R_{AA} data, can be achieved in WHDG by making the coupling a free parameter and reducing it from the $\alpha_s = 0.3$ that we take in this analysis; we refrain from such uncontrolled fitting in this paper. A quantitative estimate of the effect of allowing the coupling to run, and therefore possibly be smaller at LHC than at RHIC, requires higher order theoretical derivations that do not currently exist; in fact, even the qualitative result of such higher order effects are difficult to estimate as radiative energy loss calculations always include soft exchanges between the leading parton and the medium particles that, in principle can only be handled by nonperturbative techniques. While

one hopes that these higher order effects become small at higher leading parton momentum, there is always in heavy ion problems a temperature scale T which is the same order of magnitude as Λ_{QCD} . In particular, factorization has never been proven for energy loss calculations in heavy ion collisions. Could jet coupling to the sQGP at LHC be in fact more weakly coupled than at RHIC? From the near equality of bulk differential elliptic flow, $v_2(p_T < 2)$, the answer would appear to be no. However, for short wavelengths $p_T > 10$ GeV jet probes the effective jet medium coupling could in fact be smaller at LHC than at RHIC. The key observable to test this possibility may be the high p_T elliptic and higher flow moments[75–78], $v_2(p_T > 10 \text{ GeV}/c)$. This observable remains a key stumbling block already at RHIC for all HTL/pQCD based models including WHDG that underestimate $v_2(5 \text{ GeV}/c < p_T < 10 \text{ GeV}/c)$ significantly. If $v_2(p_T > 10 \text{ GeV}/c)$ at LHC turns out to deviate less from WHDG—even when $\alpha(LHC)$ is reduced to account for the near identity of RHIC and LHC R_{AA} —then a firmer case could be made that the sQGP at LHC is indeed more transparent to jets than expected.

In contrast to the above dynamical effects that could contribute to an apparent reduction in opacity at LHC relative to our WHDG expected growth $L/\lambda \propto (dN_{ch}/dy)^{1/3}$, there are other dynamical effects neglected in our WHDG analysis that could contribute to an apparent enhancement of the sQGP opacity at LHC:

1. High Q^2 Color Glass Condensate [68]
2. Dynamic magnetic scattering [80, 107, 108]
3. AdS/CFT holography [22, 23, 26, 27, 81]

Item 1 can be constrained via dedicated p+A and A+A direct gamma and Z boson control experiments. Cross correlating light and heavy quark flavor jet quenching systematics would provide quantitative insight into the potential influence of Items 2 and 3.

There are several other possible sources of uncertainty that we did not address here. For instance one might expect that the energy loss in confined matter would reflect the different properties of a hadronic medium as compared to a deconfined plasma of quarks and gluons [109]. Presumably, though, the cold matter energy loss would be smaller than hot, and this would lead to a greater discrepancy with the R_{cp} data. Additionally, the ordering of length scales $1/\mu \ll \lambda_{mfp} \ll L$ assumed in the DGLV energy loss derivations is violated for short length paths that may contribute more substantially to the hadrons that are ultimately observed at LHC as compared to RHIC due to the significantly more dense medium. Data from additional centrality classes will help clarify the possible role of final state confined matter effects and length scale ordering dependencies. We also mentioned previously that better calculations of the elastic energy loss of high- p_T partons exist and can additionally be improved on. Aside from the open physics issues listed above,

there is a continuing need to improve numerical evaluation algorithms to remove simplifying numerical approximations used in WHDG and other tomographic models. Due to the above considerations, experimental measurements of observables out to very high p_T , for which we demand that theoretical calculations provide a consistent picture of both the mono- and di-jet data, will be crucial for furthering our understanding of the energy loss processes in experimentally accessible quark-gluon plasma, and hence crucially important for qualitatively and quan-

titatively determining the properties of these plasmas.

VI. ACKNOWLEDGMENTS

The work of MG was supported in part by DOE Grant No. DE-FG02-93ER40764. This work was supported by the U.S. DOE under Contract No. DE-AC02-05CH11231 and within the framework of the JET Collaboration [110].

-
- [1] K. Aamodt et al. (ALICE Collab.), Phys.Lett. **B696**, 30 (2011), [arXiv:1012.1004](#).
 - [2] K. Aamodt et al. (ALICE Collab.) (2010), [arXiv:1011.3916](#).
 - [3] K. Aamodt et al. (ALICE Collab.) (2010), [arXiv:1011.3914](#).
 - [4] A. Collab. (ALICE Collab.), Phys. Rev. Lett. **106**, 032301 (2011), [arXiv:1012.1657](#).
 - [5] G. Aad et al. (ATLAS Collab.) (2010), [arXiv:hep-ex/1011.6182](#).
 - [6] S. Chatrchyan et al. (CMS) (2011), [arXiv:1102.1957](#).
 - [7] K. Adcox et al. (PHENIX), Nucl. Phys. **A757**, 184 (2005), [arXiv:nucl-ex/0410003](#).
 - [8] J. Adams et al. (STAR Collab.), Nucl.Phys. **A757**, 102 (2005), [arXiv:nucl-ex/0501009](#).
 - [9] B. B. Back et al., Nucl. Phys. **A757**, 28 (2005), [arXiv:nucl-ex/0410022](#).
 - [10] I. Arsene et al. (BRAHMS Collaboration), Nucl.Phys. **A757**, 1 (2005), [arXiv:nucl-ex/0410020](#).
 - [11] M. Gyulassy and L. McLerran, Nucl.Phys. **A750**, 30 (2005), [arXiv:nucl-th/0405013](#).
 - [12] E. V. Shuryak, Nucl.Phys. **A750**, 64 (2005), [arXiv:hep-ph/0405066](#).
 - [13] B. Muller and J. L. Nagle, Ann.Rev.Nucl.Part.Sci. **56**, 93 (2006), [arXiv:nucl-th/0602029](#).
 - [14] S. Borsanyi, G. Endrodi, Z. Fodor, A. Jakovac, S. D. Katz, et al., JHEP **1011**, 077 (2010), [arXiv:1007.2580](#).
 - [15] O. Kaczmarek, F. Karsch, E. Laermann, C. Miao, S. Mukherjee, et al., Phys.Rev. **D83**, 014504 (2011), [arXiv:1011.3130](#).
 - [16] M. Luzum and P. Romatschke, Phys. Rev. **C78**, 034915 (2008), [arXiv:0804.4015](#).
 - [17] B. Schenke, S. Jeon, and C. Gale, Phys. Rev. Lett. **106**, 042301 (2011), [arXiv:1009.3244](#).
 - [18] S. Gubser, I. R. Klebanov, and A. Peet, Phys.Rev. **D54**, 3915 (1996), [arXiv:hep-th/9602135](#).
 - [19] S. Gubser, I. R. Klebanov, and A. M. Polyakov, Phys.Lett. **B428**, 105 (1998), [arXiv:hep-th/9802109](#).
 - [20] E. Witten, Adv.Theor.Math.Phys. **2**, 505 (1998), [arXiv:hep-th/9803131](#).
 - [21] P. Kovtun, D. Son, and A. Starinets, Phys.Rev.Lett. **94**, 111601 (2005), [arXiv:hep-th/0405231](#).
 - [22] S. S. Gubser, Phys.Rev. **D74**, 126005 (2006), [arXiv:hep-th/0605182](#).
 - [23] C. Herzog, A. Karch, P. Kovtun, C. Kozcaz, and L. Yaffe, JHEP **0607**, 013 (2006), [arXiv:hep-th/0605158](#).
 - [24] C. P. Herzog, JHEP **0609**, 032 (2006), [arXiv:hep-th/0605191](#).
 - [25] J.-P. Blaizot, A. Ipp, and A. Rebhan, Annals Phys. **321**, 2128 (2006), [arXiv:hep-ph/0508317](#).
 - [26] S. S. Gubser, D. R. Gulotta, S. S. Pufu, and F. D. Rocha, JHEP **0810**, 052 (2008), [arXiv:0803.1470](#).
 - [27] P. M. Chesler, K. Jensen, A. Karch, and L. G. Yaffe, Phys.Rev. **D79**, 125015 (2009), [arXiv:0810.1985](#).
 - [28] S. S. Gubser, Nucl.Phys. **A830**, 657C (2009), [arXiv:0907.4808](#).
 - [29] P. M. Chesler and L. G. Yaffe, Phys.Rev.Lett. **106**, 021601 (2011), [arXiv:1011.3562](#).
 - [30] E. Braaten and R. D. Pisarski, Nucl. Phys. **B337**, 569 (1990).
 - [31] J. P. Blaizot, E. Iancu, and A. Rebhan, Phys. Rev. **D63**, 065003 (2001), [arXiv:hep-ph/0005003](#).
 - [32] S. S. Adler et al. (PHENIX), Phys. Rev. **C69**, 034910 (2004), [arXiv:nucl-ex/0308006](#).
 - [33] J. Adams et al. (STAR), Phys. Rev. Lett. **91**, 172302 (2003), [arXiv:nucl-ex/0305015](#).
 - [34] A. Adare et al. (PHENIX Collab.), Phys. Rev. **C77**, 064907 (2008), [arXiv:0801.1665](#).
 - [35] M. Gyulassy and M. Plumer, Phys.Lett. **B243**, 432 (1990).
 - [36] X.-N. Wang and M. Gyulassy, Phys. Rev. **D44**, 3501 (1991).
 - [37] X.-N. Wang and M. Gyulassy, Phys. Rev. Lett. **68**, 1480 (1992).
 - [38] M. Gyulassy and X.-n. Wang, Nucl. Phys. **B420**, 583 (1994), [arXiv:nucl-th/9306003](#).
 - [39] B. G. Zakharov, JETP Lett. **65**, 615 (1997), [arXiv:hep-ph/9704255](#).
 - [40] B. G. Zakharov, Phys. Atom. Nucl. **61**, 838 (1998), [arXiv:hep-ph/9807540](#).
 - [41] X.-N. Wang, Phys. Rev. **C61**, 064910 (2000), [arXiv:nucl-th/9812021](#).
 - [42] M. Gyulassy, P. Levai, and I. Vitev, Phys. Rev. Lett. **85**, 5535 (2000), [arXiv:nucl-th/0005032](#).
 - [43] M. Gyulassy, P. Levai, and I. Vitev, Nucl.Phys. **B594**, 371 (2001), [arXiv:nucl-th/0006010](#).
 - [44] U. A. Wiedemann, Nucl. Phys. **B588**, 303 (2000), [arXiv:hep-ph/0005129](#).
 - [45] R. Baier, Y. L. Dokshitzer, A. H. Mueller, and D. Schiff, JHEP **09**, 033 (2001), [arXiv:hep-ph/0106347](#).
 - [46] I. Vitev and M. Gyulassy, Phys.Rev.Lett. **89**, 252301 (2002), [arXiv:hep-ph/0209161](#).
 - [47] M. Djordjevic and M. Gyulassy, Nucl. Phys. **A733**, 265 (2004), [arXiv:nucl-th/0310076](#).
 - [48] M. Djordjevic and M. Gyulassy, Phys. Rev. **C68**, 034914 (2003), [arXiv:nucl-th/0305062](#).

- [49] M. Djordjevic, Phys. Rev. **C73**, 044912 (2006), [arXiv:nucl-th/0512089](#).
- [50] E. Wang and X.-N. Wang, Phys.Rev.Lett. **89**, 162301 (2002), [arXiv:hep-ph/0202105](#).
- [51] N. Armesto, C. A. Salgado, and U. A. Wiedemann, Phys. Rev. **D69**, 114003 (2004), [arXiv:hep-ph/0312106](#).
- [52] A. Majumder, E. Wang, and X.-N. Wang, Phys.Rev.Lett. **99**, 152301 (2007), [arXiv:nucl-th/0412061](#).
- [53] S. Wicks, W. Horowitz, M. Djordjevic, and M. Gyulassy, Nucl.Phys. **A784**, 426 (2007), [arXiv:nucl-th/0512076](#).
- [54] G.-Y. Qin, J. Ruppert, C. Gale, S. Jeon, G. D. Moore, et al., Phys.Rev.Lett. **100**, 072301 (2008), [arXiv:0710.0605](#).
- [55] N. Armesto, M. Cacciari, T. Hirano, J. L. Nagle, and C. A. Salgado, J.Phys.G **G37**, 025104 (2010), [arXiv:0907.0667](#).
- [56] A. Majumder (2009), [arXiv:0901.4516](#).
- [57] X.-F. Chen, C. Greiner, E. Wang, X.-N. Wang, and Z. Xu, Phys. Rev. **C81**, 064908 (2010), [arXiv:1002.1165](#).
- [58] M. L. Miller, K. Reygers, S. J. Sanders, and P. Steinberg, Ann.Rev.Nucl.Part.Sci. **57**, 205 (2007), [arXiv:nucl-ex/0701025](#).
- [59] D. de Florian and R. Sassot, Phys. Rev. **D69**, 074028 (2004), [arXiv:hep-ph/0311227](#).
- [60] M. Hirai, S. Kumano, and T. H. Nagai, Phys. Rev. **C76**, 065207 (2007), [arXiv:0709.3038](#).
- [61] K. J. Eskola, H. Paukkunen, and C. A. Salgado, JHEP **04**, 065 (2009), [arXiv:0902.4154](#).
- [62] J. P. Blaizot and A. H. Mueller, Nucl. Phys. **B289**, 847 (1987).
- [63] L. D. McLerran and R. Venugopalan, Phys. Rev. **D49**, 2233 (1994), [arXiv:hep-ph/9309289](#).
- [64] E. Iancu and R. Venugopalan (2003), [arXiv:hep-ph/0303204](#).
- [65] H. Weigert, Prog. Part. Nucl. Phys. **55**, 461 (2005), [arXiv:hep-ph/0501087](#).
- [66] J. Jalilian-Marian and Y. V. Kovchegov, Prog. Part. Nucl. Phys. **56**, 104 (2006), [arXiv:hep-ph/0505052](#).
- [67] L. McLerran (2008), [arXiv:hep-ph/0807.4095](#).
- [68] J. L. Albacete and C. Marquet, Phys.Lett. **B687**, 174 (2010), [arXiv:hep-ph/1001.1378](#).
- [69] W.-T. Deng, X.-N. Wang, and R. Xu, Phys. Rev. **C83**, 014915 (2011), [arXiv:1008.1841](#).
- [70] P. Levai (2011), * Temporary entry *, [arXiv:1104.4162](#).
- [71] N. Armesto, (ed.) et al., J.Phys.G **G35**, 054001 (2008), (see S. Wicks and M. Gyulassy, Sec. 7.9, Fig. 83), [arXiv:0711.0974](#).
- [72] W. A. Horowitz, Int.J.Mod.Phys. **E16**, 2193 (2007), [arXiv:nucl-th/0702084](#).
- [73] J. Noronha, M. Gyulassy, and G. Torrieri, Phys.Rev. **C82**, 054903 (2010), [arXiv:1009.2286](#).
- [74] Y. Hatta, E. Iancu, A. H. Mueller, and D. N. Triantafyllopoulos (2011), [arXiv:1102.0232](#).
- [75] R. Wei (PHENIX), Nucl. Phys. **A830**, 175c (2009), [arXiv:0907.0024](#).
- [76] C. Marquet and T. Renk, Phys. Lett. **B685**, 270 (2010), [arXiv:0908.0880](#).
- [77] J. Jia, W. Horowitz, and J. Liao (2011), [arXiv:nucl-th/1101.0290](#).
- [78] B. Betz, M. Gyulassy, and G. Torrieri (2011), [arXiv:nucl-th/1102.5416](#).
- [79] W. Horowitz and M. Gyulassy, Phys.Lett. **B666**, 320 (2008), [arXiv:nucl-th/0706.2336](#).
- [80] A. Buzzatti and M. Gyulassy, Nucl. Phys. **A855**, 307 (2011), [arXiv:1012.0614](#).
- [81] A. Ficnar, J. Noronha, and M. Gyulassy, Nucl.Phys.A in press (2010), [arXiv:1012.0116](#).
- [82] A. Adare et al. (PHENIX) (2010), [arXiv:1006.3740](#).
- [83] K. J. Eskola, H. Paukkunen, and C. A. Salgado, Nucl. Phys. **A855**, 150 (2011), [arXiv:1011.6534](#).
- [84] H. Paukkunen, C. A. Salgado, and K. J. Eskola, PoS **ICHEP2010**, 349 (2010), [arXiv:1009.3142](#).
- [85] S. S. Adler et al. (PHENIX), Phys. Rev. Lett. **94**, 232301 (2005), [arXiv:nucl-ex/0503003](#).
- [86] ATLAS-Collab. (2010), [arXiv:1012.5419](#).
- [87] X. N. Wang, private communication.
- [88] W. A. Horowitz, <https://wiki.bnl.gov/TECHQM/index.php/WHDG>.
- [89] E. Braaten and M. H. Thoma, Phys.Rev. **D44**, 2625 (1991).
- [90] S. Wicks (2008), AAT-3333486, PROQUEST-1614268891.
- [91] H. Lai et al. (CTEQ Collaboration), Eur.Phys.J. **C12**, 375 (2000), [arXiv:hep-ph/9903282](#).
- [92] B. A. Kniehl, G. Kramer, and B. Potter, Nucl. Phys. **B582**, 514 (2000), [arXiv:hep-ph/0010289](#).
- [93] A. Adare et al. (PHENIX), Phys. Rev. **D76**, 051106 (2007), [arXiv:0704.3599](#).
- [94] V. Khachatryan et al. (CMS), JHEP **02**, 041 (2010), [arXiv:1002.0621](#).
- [95] W. A. Horowitz and B. A. Cole, Phys. Rev. **C81**, 024909 (2010), [arXiv:0910.1823](#).
- [96] W. A. Horowitz and J. Jia, in preparation.
- [97] X.-F. Che, T. Hirano, E. Wang, X.-N. Wang, and H. Zhang (2011), * Temporary entry *, [arXiv:1102.5614](#).
- [98] T. Renk, H. Holopainen, R. Paatelainen, and K. J. Eskola (2011), [arXiv:1103.5308](#).
- [99] W. A. Horowitz (2010), [arXiv:1011.5965](#).
- [100] B. G. Zakharov, JETP Lett. **80**, 617 (2004), [arXiv:hep-ph/0410321](#).
- [101] S. Turbide, C. Gale, S. Jeon, and G. D. Moore, Phys. Rev. **C72**, 014906 (2005), [arXiv:hep-ph/0502248](#).
- [102] I. Vitev and B.-W. Zhang, Phys. Lett. **B669**, 337 (2008), [arXiv:0804.3805](#).
- [103] I. Vitev and M. Gyulassy, Phys. Rev. **C65**, 041902 (2002), [arXiv:nucl-th/0104066](#).
- [104] V. Topor Pop, J. Barrette, C. Gale, S. Jeon, and M. Gyulassy (2007), [arXiv:0705.2705](#).
- [105] V. Topor Pop, M. Gyulassy, J. Barrette, C. Gale, and A. Warburton, Phys. Rev. **C83**, 024902 (2011), [arXiv:1010.5439](#).
- [106] I. Vitev, Phys. Lett. **B639**, 38 (2006), [arXiv:hep-ph/0603010](#).
- [107] M. Djordjevic and U. W. Heinz, Phys. Rev. Lett. **101**, 022302 (2008), [arXiv:0802.1230](#).
- [108] M. Djordjevic, Phys. Rev. **C80**, 064909 (2009), [arXiv:0903.4591](#).
- [109] S. Domdey, B. Z. Kopeliovich, and H. J. Pirner, Nucl. Phys. **A856**, 134 (2011), [arXiv:1010.0134](#).
- [110] JET-Topical-Collaboration, <http://www.nsdth.lbl.gov/jet/>.